

Properties of cement–lime mortars vs. cement mortars containing recycled concrete aggregates

Reza Raeis Samiei^{a,*}, Bruno Daniotti^a, Renato Pelosato^b, Giovanni Dotelli^b

^a Politecnico di Milano, Dipartimento di Architettura, Ingegneria delle Costruzioni e Ambiente Costruito, Via G. Ponzio 31, 20133 Milano, Italy

^b Politecnico di Milano, Dipartimento di Chimica, Materiali e Ingegneria Chimica “Giulio Natta” and INSTM RU Polimi, p.zza L. da Vinci 32, 20133 Milano, Italy

Received 4 October 2013

Received in revised form 3 March 2015

Accepted 4 March 2015

1. Introduction

Every year many construction and demolition works are done in the world, especially in developed countries such as Europe and North America. This causes the production of a large amount of Construction and Demolition Wastes (CDW), especially in cities. In the EU27, about 869 million tons of waste were produced in 2010 [1] from the economic activity ‘Construction’ according to NACE codes [2], corresponding to about 1.7 tons per capita per year. In the United States of America, the Environmental Protection Agency (EPA) reports that the total C&D waste generation in the Northeast (the six New England States, New York and New Jersey) in 2006 was approximately 12 million tons, corresponding to roughly 0.19–0.42 tons per person per year [3].

In California, overall disposed wastes of the class of ‘Inerts and other’ amount to 11.6 million tons (29.1% of the total) and the concrete fraction is about 0.5 million tons (1.2%) [4].

In most developed countries, CDW are still mainly disposed of in landfills – either dedicated landfills or municipal solid waste (MSW) sites. However, the increasing perception of a shortage amongst natural resources [5] would suggest different practices, such as recycling the CDW again in the construction industry. One of the most effective ways to recycle CDW is to crush them into aggregates that can be reused in the production of new concrete [6]. Of course, there are severe requirements on the mechanical properties of ordinary concrete, because it generally has a structural role in buildings; therefore recycled aggregates can be used to replace natural aggregates for fabrication of concrete in limited amounts, as recent literature suggests [7–13]. For example, Evangelista & de Brito [9,10] points out that using more than 20–30% of recycled aggregates in concrete leads to a large

* Corresponding author. Mobile: +39 3299328301.

E-mail address: rosamiei@yahoo.com (R. Raeis Samiei).

increase in water absorption, due to their higher porosity when being compared to natural aggregates. Furthermore, replacement of natural aggregates with recycled aggregates can also lead to unacceptably high sulfate content in the final concrete. For a comprehensive review on the use of recycled aggregates in concrete fabrication, the reader is referred to Evangelista & de Brito [14].

Mortar is considered a less noble construction material in respect to concrete [11]; therefore there is less attention given in literature when analyzing the properties of mortars containing recycled aggregates. However, there is an increasing interest in using CDW in mortars as a replacement of natural aggregates [7–9,15–29] or binder [30]; since mortars do not have structural roles, its mechanical requirements are less stringent, and a higher amount of recycled aggregates can be used in their preparation. As pointed out by Neno et al. [28], many characteristics of the mortars containing recycled aggregates strongly depend on the quality and source of recycled aggregates and on the specific mortar composition, therefore it is expected that different outcomes emerge from different studies. In addition, using different kinds of cement can in turn affect how the binder interacts with the recycled aggregates. For example, Corinaldesi and Moriconi [25] used Portland-limestone blended cement (CEM II/B-L 32.5 R) and replaced natural sand in mortars with recycled aggregates from different sources. They discovered that the prepared mortars always had poorer mechanical strength than the reference one, but gained better mortar-brick bond strength; among the recycled aggregates used, the aggregates coming from concrete wastes led to mortars with the best performances. Braga et al. [26] instead used the fine fraction (<0.150 mm) of recycled aggregates from concrete wastes as a replacement in the preparation of mortars. They demonstrated that replacement ratios up to 15% could improve mortar performances in terms of flexural and compressive strength (increasing) and water absorption (decreasing). Unfortunately, the authors do not report details about the kind of cement used in the study. Jiménez et al. [27] replaced up to 40% by volume of natural aggregates with fine recycled aggregates obtained from ceramic partition wall rubble; they found an improvement of compressive and flexural strength of mortars made with a pozzolanic cement (CEM IV/A (V) 32.5 N), and only a small decrease in bulk density and workability of the hardened mortars. Neno et al. [28] showed that their mortars containing recycled aggregates compared well with the reference one in terms of water absorption (decreasing for replacements up to 25%) and compressive and flexural strength (increasing with replacement), while only adhesive strength was slightly poorer; also in this study the mortars were prepared using a pozzolanic cement (CEM II/B-L 32.5 N). Vegas et al. [29] used wastes from concrete and ceramic debris crushed below 2 mm in size, and suggested that a 25% replacement of fine recycled aggregates led to mortars with no loss of compressive strength, workability and shrinkage in respect to the reference mortar, using CEM II/B-M 42.5 R as binder.

Overall, as recently reviewed by Neno et al. [28] some of the effects of replacement of natural aggregates in mortars have been already understood: water absorption, density, and shrinkage characteristics. Varying results are available regarding the mechanical properties of mortars containing recycled aggregates; it seems that usually using cements with fine fillers maintains good mechanical properties in the mortars even when a high proportion of recycled aggregates are used. From the point of view of substrate adhesion, the use of concrete wastes is more advantageous in respect to other kind of wastes [25,31].

In this work, a direct comparison of cement and cement–lime mortars containing recycled aggregates was studied. Mortars prepared with high quality concrete wastes were prepared and characterized: water absorption characteristics and mechanical properties were measured, and chemical and microstructural

features of mortars have been assessed with respect to the substitution of natural with recycled aggregates and of cement with lime in the binder.

2. Materials and methods

2.1. Materials

Blended cement Type II/B-P 32.5 produced by Buzzi Unicem and hydraulic lime were used as binders. The reference natural aggregates (NA) are standard river sand aggregates with size <4 mm; the recycled aggregates (RA) have been prepared from high quality concrete wastes (Fig. 1) via a double crushing process. Sieve analyses have been done according to EN 933-1 [34] for both natural and recycled aggregates, and the results are reported in Fig. 2. The two aggregates have very different size distributions: NA particle size lies mainly around 500 μm , with neither fraction of particles below 125 μm nor above 6.25 mm. RA shows a completely different size distribution, with a large amount of coarse particles (about 70% above 5 mm) and nearly 1% of ultrafines (size <125 μm). This wide size distribution is expected to affect the mortars properties [23]; in particular, a higher filler effect is expected when using recycled aggregates, since they contain a fraction of ultrafines [35]. Sulfate acid content of the recycled aggregates was measured according to EN 1744-1 [32] and is 0.797 wt% SO_4^{2-} (less than 1% acid sulfate is recognized as an acceptable level). Water absorption of recycled aggregates is 4.5% g/g (EN 1097-6 [18]) and their apparent density is 2.67 g/cm³ (EN 1097-6 [33]), while apparent density of natural aggregates is 2.62 g/cm³.

2.2. Mix design

Eight mix batches were prepared: in four the binder was only cement (CM samples) while in the other four it was a 50:50 wt% mixture of cement and lime (CML samples).

The mix design was selected according to EN 13914-1 [36]: for CM samples, Cement:Aggregate weight ratio was 1:3 and for CLM ones the Cement:Lime:Aggregate weight ratio was 1:1:6 (see Table 1).



Fig. 1. Concrete wastes before crushing process.

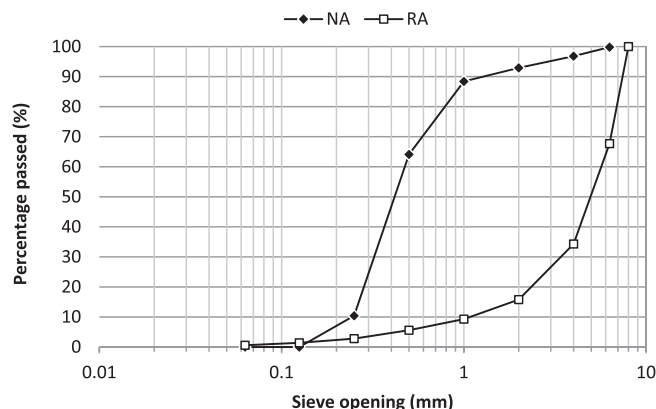


Fig. 2. Sieve size distributions of natural (filled marker, NA) and recycled (hollow marker, RA) aggregates.

The percentages of the replacement of natural aggregates with recycled ones were 0 wt% (all natural aggregates samples), 25 wt%, 50 wt%, and 100 wt% (all recycled aggregates samples). The samples name scheme will be the following: CM0, CM25, CM50 and CM100 designate cement mortars with 0%, 25%, 50% and 100% of recycled aggregates, respectively. Similarly CLM0, CLM25, CLM50 and CLM100 define cement–lime mortars with 0%, 25%, 50% and 100% of recycled aggregates, respectively. As the particle size and water absorption properties of recycled and natural aggregates are different, the substitution affected the water content in the mix design: the actual water content came out from laboratory trial tests until the viscosity of the pastes were acceptable, according to experience. The water: cement ratios of the mixes are reported in Table 1 and will agree with other reports [25]. It must be noted that the water: cement ratio has been set based on a visual observation of professional lab engineers. Since this empirical method cannot assure an exact target consistency of mortars, the increase in water need of the fresh mortars is not proportional to the amount of RA. Indeed, there is a large difference in water content between the reference samples and the ones containing the recycled aggregates in both series. However, a similar trend was observed previously, by Neno et al. [28] and accounted for the presence of fine particles in the RA that changed the mix's workability. Water absorption tests have been performed according to EN 1015-18 [37] and bulk densities of the mortars have been measured according to EN 1015-10 [38].

The mortars were cast in prismatic shapes (40 × 40 × 160 mm) for the mechanical characterization, except for the measurement of the stiffness modulus that requires cylindrical samples (diameter = 106.1 mm). All the samples were cured in air for the first 5 days and were then transferred into water until reaching 28 days of ageing.

2.3. Mechanical properties

All mechanical tests were performed on hardened mortars after 28 days of curing. Flexural strength, compressive strength, and stiffness modulus were measured. Flexural and compressive strength tests were done according to EN 1015-11 [39] and for each mix three specimens were analyzed and the average value is reported. Flexural tensile strength tests were performed with a three-support test machine on the above-mentioned prismatic samples, which were broken during the test into two parts. Then, according to the standard procedure, each half was used for the compressive strength test.

Stiffness modulus was measured according to EN 12697-26 [40] method. The tests have been performed at room temperature (about 20 °C). In this test, a hydraulic jack applies a pressure from the top, perpendicular to the cylindrical sample axis, until a fixed displacement of the jack occurs, and two sensors measure the deformation of the sample both horizontally along the cylinder axis and along its diameter (Fig. 3). Usually, the larger the displacement, the more reliable the results; yet, in some tests with the displacement set to 3 µm some of the samples broke, forcing the measurements to be done using a displacement of 2 µm. For each composition, three specimens were tested, and ten measurements were performed on each specimen; the 30 results obtained for each composition were averaged.

2.4. Chemical and microstructural characterization

Thermo-gravimetric analyses were carried out in a nitrogen atmosphere with a Seiko 6300 simultaneous TG-DTA instrument, with heating ramps of 10 °C/min. In a typical experiment, about 50 mg of sample was heated to 105 °C and kept at this temperature for 30 min to reach complete dehydration before heating up to 900 °C. Two weight losses were quantified: the stepwise loss occurring at around 500 °C, accompanying the calcium hydroxide dehydration [41], and the stepwise loss occurring nearby 750 °C, correlated to the decomposition of carbonates (mainly Calcite, CaCO₃).

The morphology of the samples was observed with a Carl Zeiss EVO50VP Scanning Electron Microscope (SEM) equipped with an Energy Dispersive Spectrometer (EDS) for elemental analysis. Both polished sections and fracture surfaces were analyzed. When needed, samples were englobated in an organic resin before polishing.

Table 1
Mix design of cement (CM) and cement–lime (CLM) mortars (weight ratios).

	CM0	CM25	CM50	CM100
C/(RA + NA)	1/3	1/3	1/3	1/3
RA/(RA + NA)	0	0.25	0.5	1
W/C	0.53	0.71	0.72	0.73
	CLM0	CLM25	CLM50	CLM100
C/L	1	1	1	1
(C + L)/(RA + NA)	1/3	1/3	1/3	1/3
RA/(RA + NA)	0	0.25	0.5	1
W/(C + L)	0.52	0.73	0.75	0.80



Fig. 3. Apparatus for the measurement of the stiffness modulus.

The X-ray powder diffraction (XRPD) data were recorded on powdered samples at room temperature, employing a Bruker D8 diffractometer using graphite-monochromated Cu-K_α radiation. The step scan was 0.02° 2θ and the measurement time of 1 s per step. The most intense peaks of Ca(OH)₂ (portlandite) and CaCO₃ (calcite) were then individually recorded with a counting time of 12 s per step. The XRD line profile analysis was made using the PeakFit™ computer program using a Pseudo-Voigt profile function. The refined profiles were used for the determination of peak positions, intensities and areas. A semi-quantitative X-ray diffraction analysis was made using the equation proposed by Copeland and Bragg [42]: $I_0/I_1 = a w_0/w_1$. I_0 and I_1 are the integrated intensities of the XRD lines of two components in a mixture, w_0 and w_1 are their weight fractions and 'a' is a proportionality constant.

3. Results

3.1. Mechanical properties of 28 days cured mortars

3.1.1. Compressive and flexural strength

Fig. 4 reports the results of the compressive and flexural tensile strength obtained on CM samples. The measured compressive strength of cement containing mortars (CM) is comparable with previous results reported by Corinaldesi and Moriconi [25] for concrete wastes. Compressive strength decreases upon increasing the content of recycled aggregates (Fig. 4, filled marker) from about

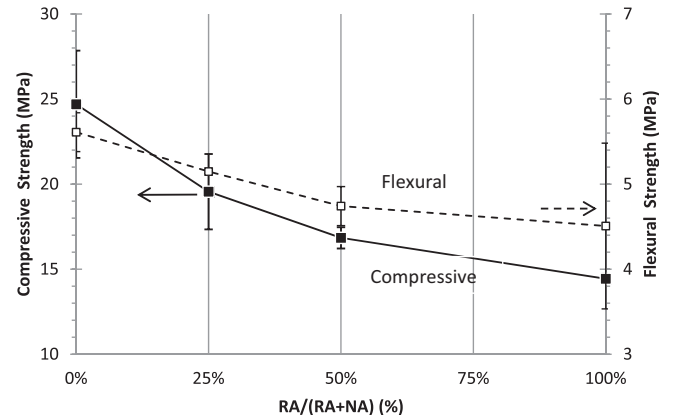


Fig. 4. Compressive (filled marker, left axis) and flexural (hollow marker, right axis) strength of CM samples.

25 MPa in CM0 to about 15 MPa in CM100; both absolute values and magnitudes of the decrease in strength are in agreement with those already reported [25]. Flexural strength has a similar decrease (Fig. 4, hollow markers).

Fig. 5 illustrates the results obtained with CLM samples: the mechanical performances are much poorer than those of the equivalent CM samples. In addition, compressive and flexural strength increase when increasing the proportion of recycled aggregates. Compressive strength increases from about 5 MPa in CLM0 to nearly 8 MPa in CLM100 (about a 60% increase). The largest strength increase is reported from a 25% to 50% replacement, and then the compressive strength remains similar in the 100% RA sample. Flexural strength shows a parallel increase, except for the fact that the strength increment from 0% to 50% substitution is linear.

3.1.2. Stiffness modulus

Fig. 6 shows the results of the stiffness modulus measurements. The results obtained with CM samples are substantially higher than those with CLM samples are; in agreement with the compressive and flexural strength results, the effect of the increasing amount of recycled aggregates is the opposite in the two series: in CM samples, the stiffness modulus decreases when increasing the amount of RA in the mortar. Instead, stiffness increases when increasing the amount of RA in the CLM series. Thou, the biggest variation in the stiffness value occur when changing from 0% RA to 25% RA; then, the value remains nearly constant at higher RA contents. It is worth noting that this particular trend seems to mimic the progress of water:cement ratios in the samples. Stiffness Modulus for CM decreases about 16% from CM0 to CM100 and increases about 27% from CLM0 to CLM100.

3.2. Bulk dry density of hardened mortars

Fig. 7 illustrates the variation of the bulk dry densities of the prepared samples with respect to the amount of recycled aggregates. The density is greater in cement mortars (CM) than in cement–lime mortars (CLM). In both series, increasing the amount of recycled aggregates causes a reduction in the final sample density: in the CM series it drops about 6% from 2079 kg/m³ (CM0) to 1947 kg/m³ (CM100); in the CLM series it decreases 4% from 1808 kg/m³ (CLM0) to 1736 kg/m³ (CLM100). Since the bulk densities of the natural and recycled aggregates are very close to each other (2.62 g/cm³ for NA and 2.67 g/cm³ for RA), the result is somewhat unexpected. The microstructural evolution during hydration must then be responsible for the observed decrease rather than a trivial mixture effect.

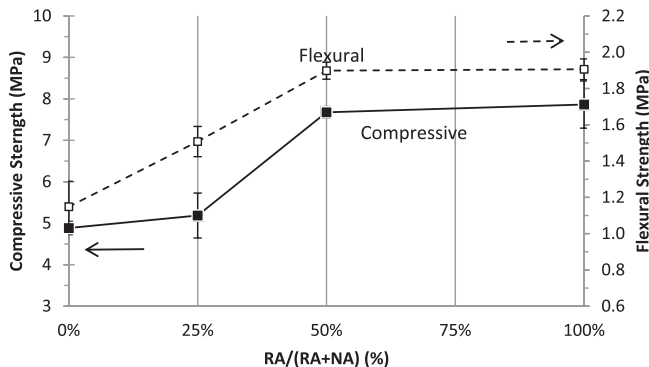


Fig. 5. Compressive (filled marker, left axis) and flexural (hollow marker, right axis) strength of CLM samples.

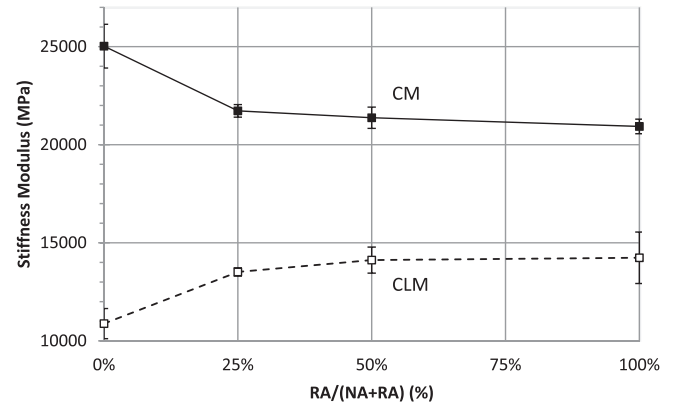


Fig. 6. Stiffness modulus of cement (CM, filled marker) and cement–lime (CLM, hollow marker) mortars.

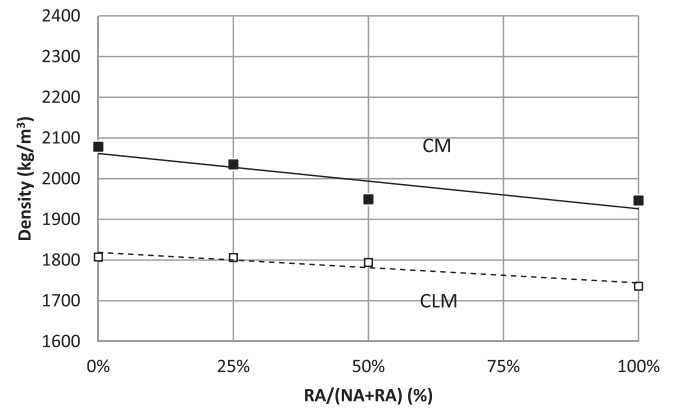


Fig. 7. Bulk density of CM (filled marker) and CLM (hollow marker) vs. substitution of aggregates.

3.3. Water absorption of hardened mortars

Fig. 8 reports the results of the water absorption tests. The samples were placed in water using a paraffin layer to protect five of its six faces: water absorption (C) was then calculated according to the following equation:

$$C = 0.1(M2 - M1)[\text{kg}/(\text{m}^2 \cdot \text{min}^{0.5})] \quad (1)$$

where M1 is the mass in kg of the specimen after 10 min in water and M2 is the mass in kg of the specimen after 90 min in water.

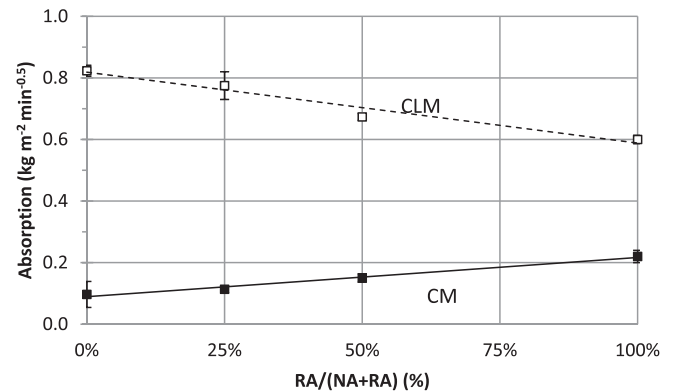


Fig. 8. Water absorption of hardened mortars.

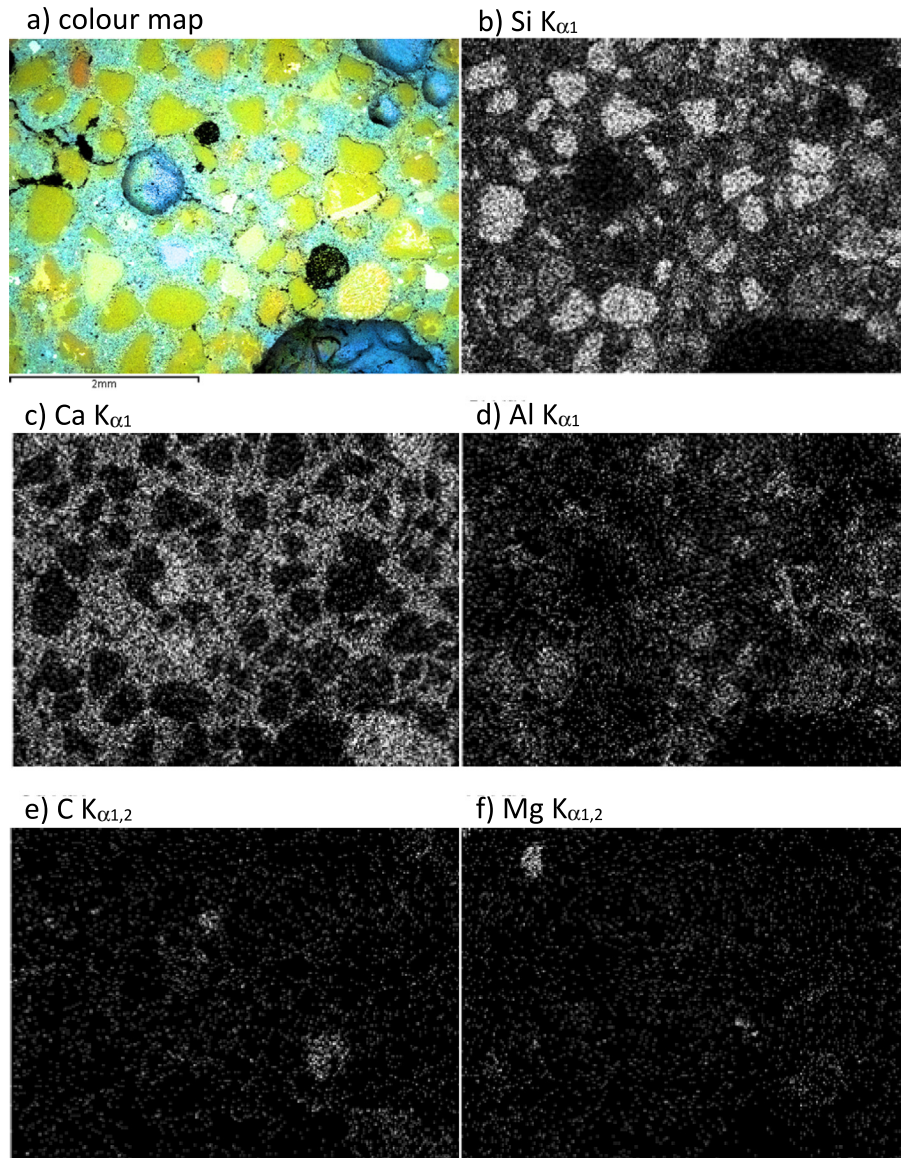


Fig. 9. (a) colour SEM-EDS map of CM0 sample obtained by combining the single EDS element maps reported in (b)–(f). (For interpretation of the references to colour in this figure legend, the reader is referred to the web version of this article.)

Overall, water absorption is quite low in both series. Water absorption is lower in CM samples with respect to CLM ones. Furthermore, increasing the amount of RA affects the water absorption of CM and CLM samples in opposite ways: in CM series, the amount of absorbed water increases with increasing RA content, while the opposite occurs in CLM samples. In details, the increase in water absorption occurring in CM series seems to be a mere effect of the higher water absorption of the recycled aggregates in respect to the natural ones. When observing CLM mortars, the amount of absorbed water diminishes when increasing the amount of RA. This result seems counterintuitive, but a couple of explanations can be articulated. (i) The RA added in the mix adhered some old mortar that already has a high hydration degree; possibly, this mortar is less porous than the matrix of the CLM itself. (ii) The higher hydraulicity of the binder in the CLM samples, together with the fine fraction of recycled aggregates, could promote a superior bonding between the binder and the recycled aggregates, limiting the capillary porosity. The microscopic observations below (Section 3.4.1, Fig. 12) seem to support these facts.

Interestingly, the water absorption behavior fairly mimics the trend found in the mechanical strength tests.

3.4. Microstructure and composition

3.4.1. Microstructure

Figs. 9–11 show the scanning electron microscope micrographs of the two series of samples. All the images were recorded using the backscattered electrons signal, in which the brightness of the different parts of the image is related to the chemical composition rather than to the topography of the sample. Fig. 9 serves as a guideline and reports the composition map of the CM0 sample (Fig. 9a) and the concentration maps of the various elements (Fig. 9b–f, the brighter the spot, the higher the concentration of the element in that spot). The single maps were used to colorize Fig. 9a where all the chemical information is combined in a single image. Maps of Fe, Na and K are omitted for clarity. The colour code is the following: green = silicon, blue = calcium, white = aluminium and iron, red = magnesium, black = carbon. Parts with higher

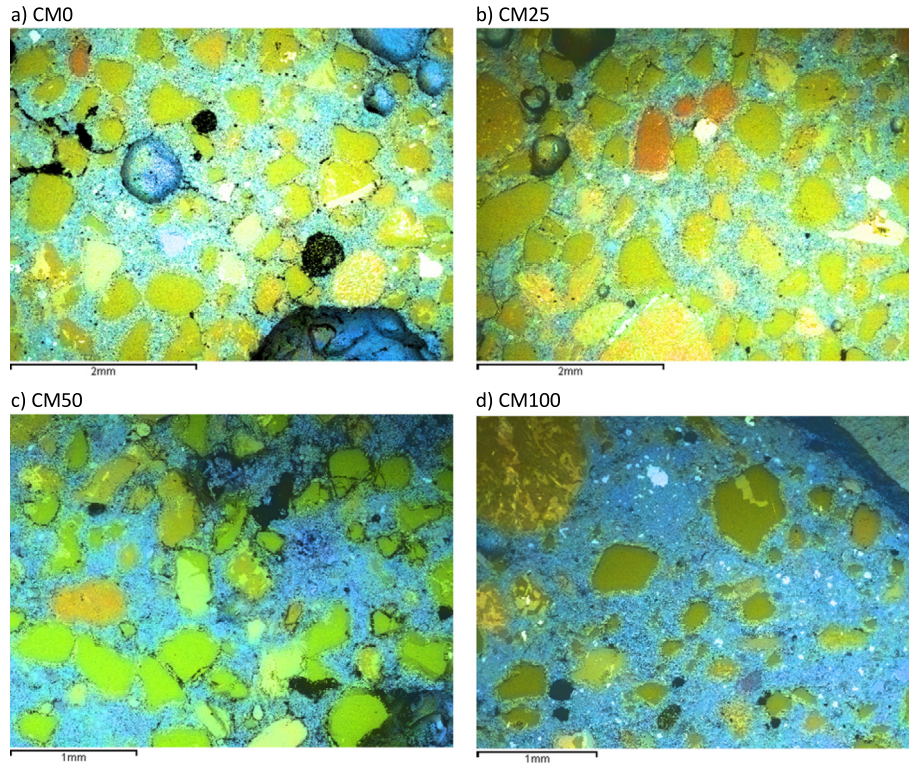


Fig. 10. SEM micrographs of CM samples.

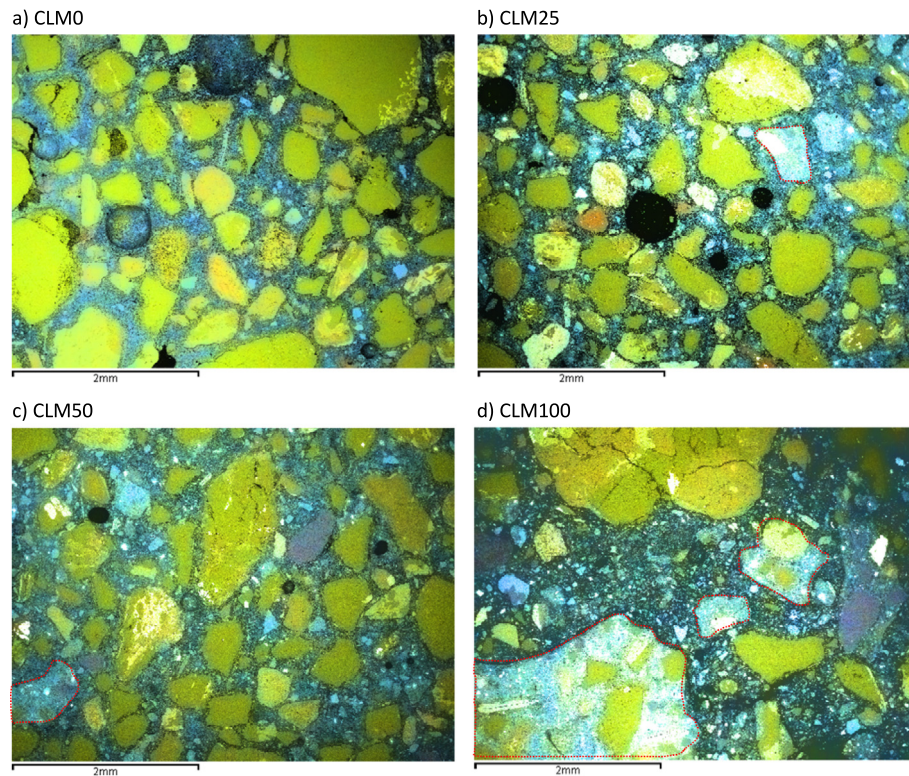


Fig. 11. SEM micrographs of CLM samples.

colour saturation in the image correspond to spots with higher concentration of the corresponding element in the sample.

Fig. 10 shows the obtained maps for the CM series: in CM0 (Fig. 10a) the green-yellowish grains belong to natural aggregates

(rich in silicon) and their size distribution seem to be in agreement with the sieve analyses (from a few hundreds of micrometres to 1 mm size). The light blue matrix contains the hydrated cement phases and CaCO_3 (calcium rich phases). Some black spots of

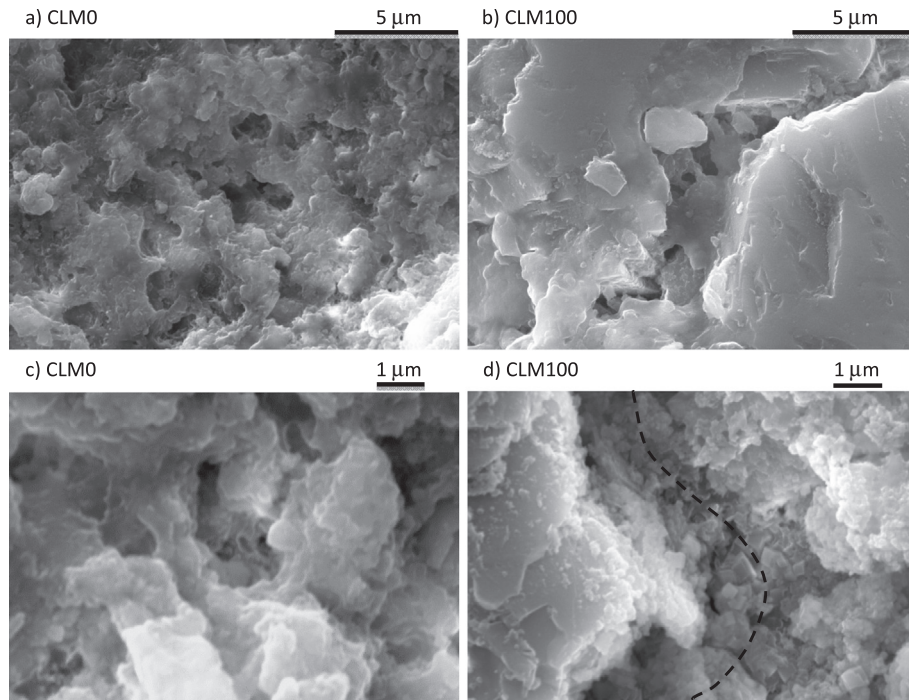


Fig. 12. High resolution SEM images of CLM0 (a, c) and CLM100 (b, d) samples; the dashed line shows the binder–aggregate boundary region.

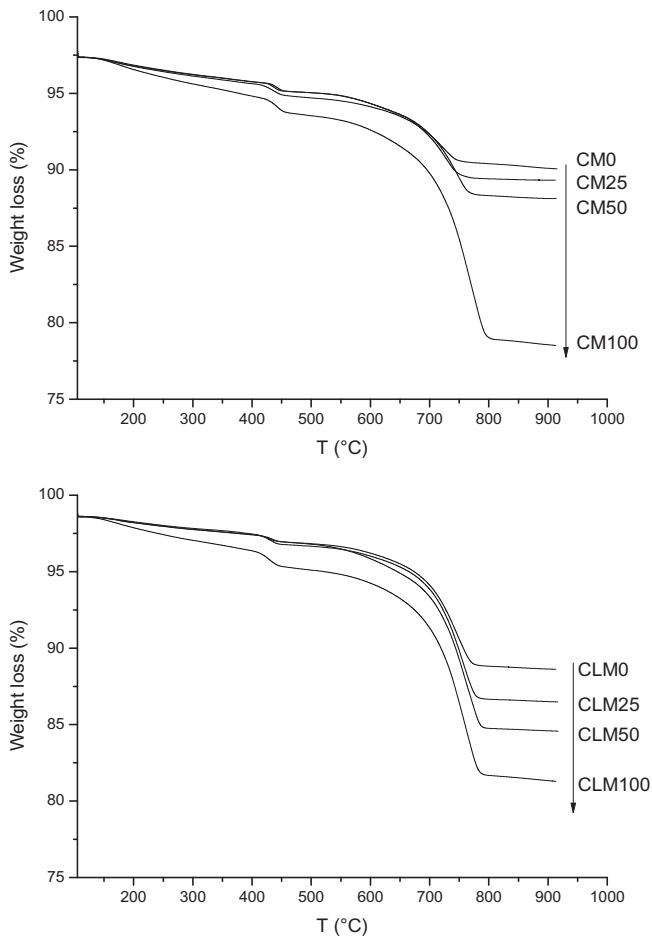


Fig. 13. TG curves of (a) CM and (b) CLM samples (normalized at 105 °C).

carbonaceous nature deriving from the pozzolanic portion of the starting cement are also observed. A few circular blue features are likely to be cavities arising from air bubbles formed during the mixing process or voids left by the removal of aggregate particles during the polishing process. The distribution of the aggregates is similar in all the samples, but the amount of the silicon rich grains decreases as the amount of recycled aggregates increases. Indeed, in the recycled aggregates the silicate sand carries a lot of hydrated cement paste, so that the fraction of calcium rich phases in the samples increases as the amount of RA increases.

Fig. 11 reports the SEM micrographs of the CLM series: in CLM0 (Fig. 11a) as in CM0 before the cement matrix (in blue) bind the natural aggregates (green-yellowish grains), which size distribution is in agreement with the sieve analyses. Small carbonaceous particles and cavities are also visible. As the amount of recycled aggregates in the sample increases (Fig. 11b–d), it is easier to observe blocks of hydrated mortar stemming from the recycled aggregates. It is not usually easy to determine the boundary of recycled aggregate blocks, but Fig. 11b–d show a tentative identification of a few light blue blocks, highlighted with dotted red outlines.

Fig. 12 shows high resolution images of fracture surfaces of samples CLM0 and CLM100: Fig. 12a and b illustrate the binder matrix microstructure: in CLM0 (Fig. 12a) the apparent porosity

Table 2

Portlandite and calcite amounts in cement (CM) and cement–lime (CLM) mortars as a function of aggregate replacement (calculated from TG measurements).

	CM0	CM25	CM50	CM100
Portlandite (wt%)	3.9	3.0	3.1	5.5
Calcite (wt%)	10	19	16	35
	CLM0	CLM25	CLM50	CLM100
Portlandite (wt%)	3.5	3.2	2.5	6.9
Calcite (wt%)	18	23	28	31

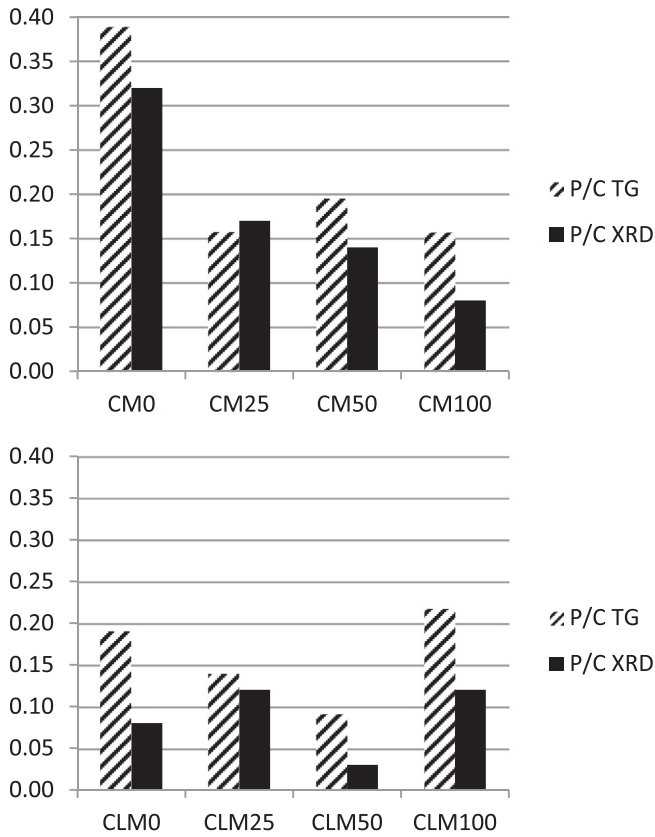


Fig. 14. Portlandite/calcite ratios calculated via TG and XRD techniques.

is much larger than in CLM100 (Fig. 12b). The latter developed a more compact microstructure that could be responsible for the mechanical properties and water absorption behavior reported above (Sections 3.1 and 3.3). Figs. 12c and d instead illustrate the difference between the porosity in CLM0 (Fig. 12c) and the compactness of CLM100, where the growth of many small crystals hindered the pores in the binder–aggregate interface (Fig. 12d, the dashed line indicates the binder–aggregate boundary).

3.4.2. Thermogravimetric analysis

A Thermo-gravimetric analysis has been performed on all samples to estimate the amount of portlandite and calcite in the specimens. Fig. 13 illustrates the TG curves of (a) CM and (b) CLM series. There is a small weight loss in all plots at about 440 °C; this stepwise loss is usually attributed to the dehydration of Ca(OH)_2 [41] and has been used for the quantification of its amount in the samples. Table 2 summarizes the obtained results: Ca(OH)_2 amounts increase stepping from mortar containing only natural aggregate to the one containing only recycled aggregate, both in CM and CLM series. In detail, Ca(OH)_2 amounts increase from 3.9 wt% in CM0 to 5.5 wt% in CM100 and from 3.5 wt% in CLM0 to 6.8 wt% in CLM100. The decomposition of carbonate species was estimated as well, by quantification of the stepwise loss occurring at 700–800 °C (see Table 2) and converted to the corresponding CaCO_3 amount in the mortar: it increases from 10 wt% in CM0 to 35 wt% in CM100, and from 18 wt% in CLM0 to 31 wt% in CLM100.

Fig. 14 reports the portlandite:calcite ratios obtained from the thermogravimetric analysis, together with the ones calculated from XRD data. The ratio is utilized here to allow for the comparison with the data obtained from the XRD measurements since it is a challenging task to calculate the absolute amount of two components in a multi-phase mixture, while their ratios can be extracted quite easily with good reliability. In the cement mortars

(CM) the ratio of Portlandite:calcite strongly decreases stepping from the sample containing only natural aggregates to the one with recycled aggregates, and then changes much less by adding more recycled aggregates. Overall, in the cement–lime mortars (CLM) the ratio is lower, and the trend is not monotonic: the ratio decreases up to 50% substitution to increase again at 100% substitution.

3.4.3. X-ray diffraction analysis

X-ray diffraction analysis of the most intense peaks of portlandite and calcite in the mortars (see Fig. 15) allowed relating the ratio of the two peak areas with the ratio of the amount of the two components in the mixture, by using Eq. (1) (Section 2.3). The proportionality constant a in Eq. (1) has been calculated using the standardless method of the Reference Intensity Ratios (RIR).

The portlandite:calcite ratio strongly decreases when increasing the recycled aggregates in CM series, while it slightly increases in the CLM series (Fig. 14). Moreover, Fig. 14 underlines that the trend of the portlandite:calcite ratio can be estimated by both TG and XRD analysis, and shows a fair correlation with the mechanical properties results.

4. Discussion

A common outcome when replacing natural aggregates in a mortar with recycled aggregates is a decrease in strength and an increase in water penetration [25], especially when more than 30% of natural aggregates are replaced with recycled ones. The results obtained in this research will conform to this statement if we take into account the mortars prepared with cement binder (CM series). On the contrary, when the binder is a 50:50 wt% mixture of hydraulic lime and cement (CLM series), the prepared mortars show an increase of their compressive strength of up to 60% and a decrease in water absorption as a result of the substitution. Still, the overall properties are largely worse (i.e., reduced strength and higher water absorption) than those of the homologue CM samples.

Table 2 reports the amount of Ca(OH)_2 (a product of the binder hydration reactions), and of CaCO_3 in the samples, as calculated via Thermogravimetric techniques. By comparing the amount of Ca(OH)_2 and CaCO_3 measured in the aged samples with the ones expected from the mass balance of the starting materials, we can draw some conclusions about the mortars hydration reactions. In sample CM0 the only source of Ca(OH)_2 is the normal hydration reaction of the cement binder. In samples CM25, CM50 and CM100 there are two sources: (i) Ca(OH)_2 produced by the hydration reaction of cement, and (ii) Ca(OH)_2 already present in the recycled aggregates (estimated at about 2% via TG analysis, not reported here). Thus, if we suppose that hydration reactions occur at the same rate in all the samples, we expect that Ca(OH)_2 in the samples increase monotonically in the order $\text{CM} < \text{CM25} < \text{CM50} < \text{CM100}$. Of course some of the Ca(OH)_2 can also be consumed by side reactions; these are (i) Ca(OH)_2 carbonation reaction to give CaCO_3 and (ii) pozzolanic reaction. By the way, the latter one is usually much slower than hydration and is not expected to affect the amount of Ca(OH)_2 after 28 days of curing [43]. Assuming that carbonation occurs at the same rate in all the samples, the amount of Ca(OH)_2 consumed by carbonation should be proportional to the starting amount, and therefore should not affect the trend reported above. For what concerns CaCO_3 , its amount is expected to increase monotonically in the same way ($\text{CM0} < \text{CM25} < \text{CM50} < \text{CM100}$) because RA themselves contain a fixed amount (about 25% calculated via TG analysis) of

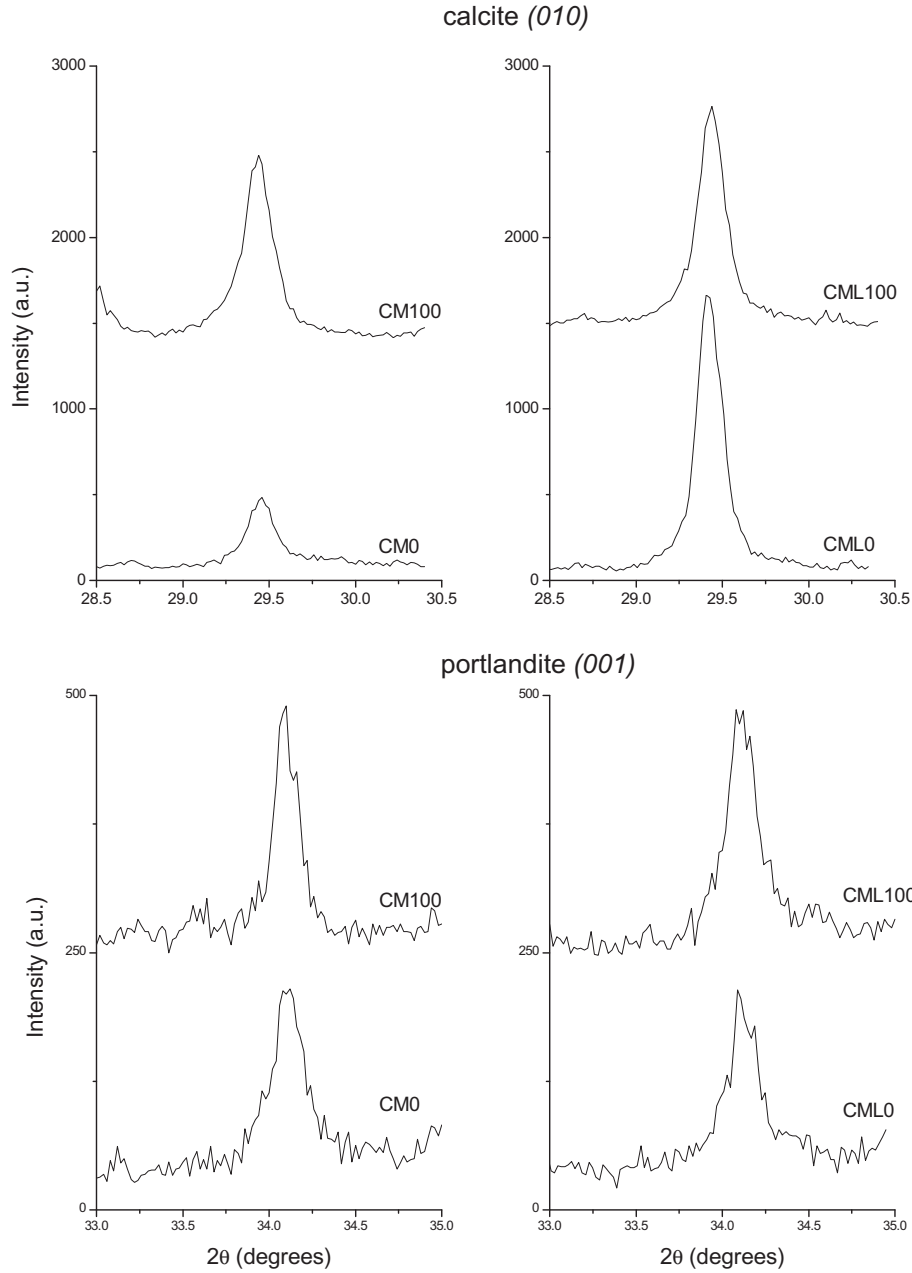


Fig. 15. XRD of individual peaks of calcite and portlandite used for the semi-quantitative analysis.

CaCO_3 . The amount of CaCO_3 formed by Ca(OH)_2 carbonation should be negligible and not modify this trend.

In cement–lime mortars (CLM), the sources of Ca(OH)_2 are: (i) cement hydration and (ii) Ca(OH)_2 from lime in CLM0 sample. In CLM25, CLM50 and CLM100 sources of Ca(OH)_2 are (i) cement hydration, (ii) Ca(OH)_2 from lime and (iii) Ca(OH)_2 already present in the recycled aggregates (about 2% of RA). The reactions consuming Ca(OH)_2 are the same as for CM series, and therefore the same increase in Ca(OH)_2 is therefore expected in the end. Again, the CaCO_3 amount is expected to increase monotonically in the CML0–CML25–CML50–CML100 series because RA contain a fixed amount (about 25%) of CaCO_3 , and the CaCO_3 arising from Ca(OH)_2 carbonation should not substantially affect the total amount.

Overall, the experimental results are in agreement with this scheme for what concerns CaCO_3 : its amount increases in both

series, and its content is higher in the CLM series where hydraulic lime replaces half of the cement as binder. Only in samples containing 100% RA is the amount of CaCO_3 is comparable between the two series (see Section 3.2 and Table 2).

Despite the fact that in CLM series there is a lot more Ca(OH)_2 present in the starting mixture (50% of the binder is lime), the final amounts of Ca(OH)_2 in the two series are comparable. It can be expected that this missing Ca(OH)_2 can be responsible for the promotion of the strength increase in the CLM series. The microstructural evidences seem to suggest that CLM samples develop a denser microstructure as a result of the RA addition (witnessed by the decreased water absorption, see Fig. 8). This microstructure could be the reason for the positive effect on the strength of the CLM mortars. It is possible that this promotion arises from a synergic effect of the lime and pozzolana in the binder with the hydrated cement paste in the recycled aggregates. The trend of the

portlandite/calcite ratio for these mixtures could be a quick indicator of the relative hydration degree of the samples, which in turn relates to the strength of the aged mortars.

5. Conclusions

The purpose of this research is to understand how the replacement of natural aggregates with recycled aggregates could affect the mechanical performances of mortars. Four mix designs using cement binder and four using cement–lime binder were prepared in this study. As expected, the mechanical properties of cement mortars are always better than those of cement–lime mortars. The effect of replacing natural aggregates with recycled ones on the mechanical properties and on water absorption are inverse in the two series: when the binder is cement the mechanical properties worsen and water absorption increases by increasing RA content. Surprisingly, the opposite occurs when the mortar is prepared using a 50:50 wt% mixture of cement and lime as the binder.

The main outcomes of this experimental work are:

- The samples have been made with the constant Consistency. Water content is increasing dramatically between 0% recycled aggregates to 25% recycled aggregates for both series (CLM and CM).
- The recycled aggregates mortars with lime cement binders (CLM) show an increase in compressive strength up to 60% when increasing the portion of recycled aggregates (RA/(RA + NA)). The Flexural tensile strength shows a similar increase up to 50% substitution. Stiffness modulus increases from 10,000 MPa to 14,000 MPa.
- The recycled aggregates mortars with only cement binder (CM) show a noticeable decrease in mechanical performances, as already reported in the literature. The compressive strength decreases from 25 MPa to 15 MPa, and flexural tensile strength decreases from 5.8 MPa to 3.9 MPa when substituting the natural aggregates with the recycled ones. The stiffness modulus decreases in the same way from 25,000 MPa to 21,000 MPa.
- Of the 8 prepared mix designs, 6 of them are in class IV (CM0, CM25, CM50, CM100, CLM50 and CLM100), and two of them (CLM0 and CLM25) are in class III according to EN 998-1 [44].
- The water absorption of CLM samples decreases when increasing the fraction of recycled aggregates from $0.8 \text{ kg m}^{-2} \text{ min}^{-0.5}$ to $0.6 \text{ kg m}^{-2} \text{ min}^{-0.5}$. However, increasing the fraction of recycled aggregates in the CM series instead causes an increase in water absorption from $0.05 \text{ kg m}^{-2} \text{ min}^{-0.5}$ to $0.21 \text{ kg m}^{-2} \text{ min}^{-0.5}$.
- The bulk density of samples decrease when increasing the fraction of recycled aggregates: from 2100 kg/m^3 to 1950 kg/m^3 in CM series, and from 1800 kg/m^3 to 1748 kg/m^3 in CLM series.
- TG and XRD analyses showed that the trend of the ratio of portlandite and calcite in the samples as a function of the added recycled aggregates fairly follows the trend of the mechanical properties.

References

- [1] Eurostat. Waste generation and management. European Commission; 2010.
- [2] Eurostat. NACE rev. 2 – statistical classification of economic activities in the European Community; 2008. p. 363.
- [3] NEWMOA. Construction & demolition waste management in the northeast in 2006; 2009.
- [4] California Integrated Waste Management Board. California 2008 statewide waste characterization study – significant tables and figures; 2009.
- [5] Krausmann F, Gingrich S, Eisenmenger N, Erb K-H, Haberl H, Fischer-Kowalski M. Growth in global materials use, GDP and population during the 20th century. *Ecol Econ* 2009;68(10):2696–705.
- [6] UEFG. Study on data needs for a full raw materials flow analysis; 2012.
- [7] Corinaldesi V, Moriconi G. Influence of mineral additions on the performance of 100% recycled aggregate concrete. *Constr Build Mater* 2009;23(8):2869–76.
- [8] Sales A, de Souza FR. Concretes and mortars recycled with water treatment sludge and construction and demolition rubble. *Constr Build Mater* 2009;23(6):2362–70.
- [9] Evangelista L, de Brito J. Environmental life cycle assessment of concrete made with fine recycled concrete aggregates. In: SB07 Lisbon – sustainable construction, materials and practices: challenge of the industry for the new millennium. Rotterdam (Netherlands): In-House Publishing; 2008. p. approx. 6.
- [10] Evangelista L, de Brito J. Criteria for the use of fine recycled concrete aggregates in concrete production. In: Vázquez E, Hendriks CF, Janseen GMT, editors. International RILEM conference on the use of recycled materials in building and structures. Barcelona, Spain: RILEM Publications SARL; 2004.
- [11] Pereira P, Evangelista L, de Brito J. The effect of superplasticisers on the workability and compressive strength of concrete made with fine recycled concrete aggregates. *Constr Build Mater* 2012;28(1):722–9.
- [12] Thomas C, Sosa I, Setién J, Polanco JA, Cimentada AI. Evaluation of the fatigue behavior of recycled aggregate concrete. *J. Cleaner Prod* 2014;65:397–405.
- [13] Andreu G, Miren E. Experimental analysis of properties of high performance recycled aggregate concrete. *Constr Build Mater* 2014;52:227–35.
- [14] Evangelista L, de Brito J. Concrete with fine recycled aggregates: a review. *Eur J Environ Civ Eng* 2014;18(2):129–72.
- [15] Mas B, Cladera A, Olmo TD, Pitarch F. Influence of the amount of mixed recycled aggregates on the properties of concrete for non-structural use. *Constr Build Mater* 2012;27(1):612–22.
- [16] Higashiyama H, Yagishita F, Sano M, Takahashi O. Compressive strength and resistance to chloride penetration of mortars using ceramic waste as fine aggregate. *Constr Build Mater* 2012;26(1):96–101.
- [17] Caballero J, Polder RB, Fraaij ALA. Chloride penetration into cementitious mortar at early age. *Heron* 2012;57(3):185–96.
- [18] Miranda LFR, Selmo SMS. CDW recycled aggregate renderings: Part II – analysis of the effect of materials finer than $75 \mu\text{m}$ under accelerated aging performance. *Constr Build Mater* 2006;20(9):625–33.
- [19] Miranda LFR, Selmo SMS. A case study on the variation of the quality of mortars using CWD recycled sands. In: Vázquez E, Hendriks CF, Janseen GMT, editors. International RILEM conference on the use of recycled materials in building and structures. Barcelona, Spain: RILEM Publications SARL; 2004.
- [20] Shui Z, Xuan D, Wan H, Cao B. Rehydration reactivity of recycled mortar from concrete waste experienced to thermal treatment. *Constr Build Mater* 2008;22(8):1723–9.
- [21] de Aguiar G, Selmo SMS. An initial analysis of the effect of gypsum plaster in recycled fine aggregates from C&D wastes. In: Vázquez E, Hendriks CF, Janseen GMT, editors. International RILEM conference on the use of recycled materials in building and structures. Barcelona, Spain: RILEM Publications SARL; 2004. p. 493–502.
- [22] Hammond GP, Jones CI. Embodied energy and carbon in construction materials. *Proc Inst Civ Eng Energy* 2008;161(2):87–98.
- [23] Silva J, de Brito J, Veiga R. Recycled red-clay ceramic construction and demolition waste for mortars production. *J Mater Civ Eng* 2010;22(3):236–44.
- [24] Silva J, Brito J, Veiga R. Fine ceramics replacing cement in mortars partial replacement of cement with fine ceramics in rendering mortars. *Mater Struct* 2007;41(8):1333–44.
- [25] Corinaldesi V, Moriconi G. Behaviour of cementitious mortars containing different kinds of recycled aggregate. *Constr Build Mater* 2009;23(1):289–94.
- [26] Braga M, de Brito J, Veiga R. Incorporation of fine concrete aggregates in mortars. *Constr Build Mater* 2012;36:960–8.
- [27] Jiménez JR, Ayuso J, López M, Fernández JM, de Brito J. Use of fine recycled aggregates from ceramic waste in masonry mortar manufacturing. *Constr Build Mater* 2013;40:679–90.
- [28] Neno C, de Brito J, Veiga R. Using fine recycled concrete aggregate for mortar production. *Mater Res* 2013;17(1).
- [29] Vegas I, Azkarate I, Juarrero A, Frías M. Design and performance of masonry mortars made with recycled concrete aggregates [Diseño y prestaciones de morteros de albañilería elaborados con áridos reciclados procedentes de escombros de hormigón]. *Mater Construcc* 2009;59(295):5–18.
- [30] Florea MVA, Ning Z, Brouwers HJH. Activation of liberated concrete fines and their application in mortars. *Constr Build Mater* 2014;50:1–12.
- [31] Moriconi G, Corinaldesi V, Antonucci R. Environmentally-friendly mortars: a way to improve bond between mortar and brick. *Mater Struct* 2003;36(10):702–8.
- [32] European Committee for Standardization – CEN. EN 1744-1 tests for chemical properties of aggregates Part 1: chemical analysis; 2012.
- [33] European Committee for Standardization – CEN. EN 1097-6 tests for mechanical and physical properties of aggregates Part 6: determination of particle density and water absorption; 2013.
- [34] European Committee for Standardization – CEN. EN 933-1 Tests for geometrical properties of aggregates – Part 1: determination of particle size distribution – sieving method; 2012.
- [35] Correia JR, de Brito J, Pereira AS. Effects on concrete durability of using recycled ceramic aggregates. *Mater Struct [Materiaux et Constructions]* 2006;39(286):169–77.
- [36] European Committee for Standardization – CEN. EN 13914-1 design, preparation and application of external rendering and internal plastering Part 1: external rendering; 2005.

- [37] European Committee for Standardization – CEN. EN 1015-18 methods of test for mortar for masonry determination of water absorption coefficient due to capillary action of hardened mortar; 2004.
- [38] European Committee for Standardization – CEN. EN 1015-10 methods of test for mortar for masonry Part 10: determination of dry bulk density of hardened mortar; 2007.
- [39] European Committee for Standardization – CEN. EN 1015-11 methods of test for mortar for masonry Part 11: determination of flexural and compressive strength of hardened mortar; 2007.
- [40] European Committee for Standardization – CEN. EN 12697-26 bituminous mixtures – test methods for hot mix asphalt – Part 26: stiffness; 2012.
- [41] Midgley HG. The determination of calcium hydroxide in set Portland cements. *Cem Concr Res* 1979;9(1):77–82.
- [42] Copeland LE, Bragg RH. Quantitative X-ray diffraction analysis. *Anal Chem* 1958;30(2):196–201.
- [43] Papadakis VG, Fardis MN, Vayenas CG. Hydration and carbonation of pozzolanic cements. *ACI Mater J* 1992;89(2):119–30.
- [44] European Committee for Standardization – CEN. EN 998-1 specification for mortar for masonry – Part 1: rendering and plastering mortar; 2010.